Printed in the Republic of Korea
ANALYTICAL SCIENCE & TECHNOLOGY
Vol. 24, No. 2, 78-84, 2011

Electrospray ionization tandem mass fragmentation pattern of camostat and its degradation product, 4-(4-guanidinobenzoyloxy)phenylacetic acid

Soonho Kwon, Hye-Jin Shin, Jimyeong Park, Kyoung-Ryul Lee, Young-Jin Kim and Sanghoo Lee★

Department of Bioanalysis, Seoul Medical Science Institute & Seoul Clinical Laboratories, Seoul 152-766, Korea

(Received October 1, 2010; Accepted March 3, 2011)

Camostat 및 분해산물 4-(4-guanidinobenzoyloxy)phenylacetic acid의 전자분무 이온화 텐덤 질량 fragmentation 패턴

권순호 · 신혜진 · 박지명 · 이경률 · 김영진 · 이상후★

(재)서울의과학연구소 질량분석부

(2010. 10. 1. 접수, 2011. 3. 3. 승인)

Abstract: The fragmentation patterns of a serine protease inhibitor, camostat, and its degradation product, 4-(4-guanidinobenzoyloxy)phenylacetic acid (GBPA), were for the first time investigated by a triple quadrupole tandem mass spectrometry equipped with an electrospray source (ESI-MS/MS) in positive and/or negative ion mode under collision-induced dissociation (CID). The positive CID spectrum of camostat showed distinctly that the single bond (C-O) cleavage between carbonyl group and oxygen atom of the ester bonds of the compound favorably occurred and then the loss of *N*,*N*-dimethylcarbamoylmethyl group was more susceptible than that of guanidine moiety. In the positive ion CID spectrum of GBPA, the initial cleavage between the carbonyl group and oxygen atom of 4-guanidinobenzoyloxy group also occurred, yielding the most abundant fragment ion at *m/z* 145. On the other hand, the negative CID spectrum of GBPA characteristically showed the occurrence of the most abundant peak at *m/z* 226 resulting from the sequential neutral losses of CO_2 and HN=C=NH from the parent ion at *m/z* 312.

요 약: 본 연구에서는 양성 및/또는 음성 이온 방식으로 저에너지 충돌-유발 분해(CID)를 이용한 serine protease 저해제인 camostat 와 그것의 분해산물인 4-(4-guanidinobenzoyloxy)phenylacetic acid (GBPA)의 분해 패턴을 전자분무 소스가 있는 사중극자 텐덤 질량분석기(ESI-MS/MS)를 이용하여 최초로 조사하였다. Camostat의 양이온 CID 질량 스펙트럼 분석결과, 분자구조내 에스테르 결합을 이루는 카르보닐 기와 산소 원자사이의 단일 결합(C-O) 분해가 우선적으로 일어나고, guanidine 기의 초기 손실보다는 *N*,*N*-dimethylcarbamoylmethyl 기의 초기 손실이 더 잘 일어난다는 것이 특징적으로 확인되었다. GBPA의 양이온 CID 스펙트럼의 경우는, 4-guanidinobenzoyloxy 기에 있는 카르보닐 기와 산소원자 사이의 초기 분

★ Corresponding author
Phone : +82-(0)70-7115-8697 Fax : +82-(0)2-858-2814
E-mail : sprout30@scllab.co.kr

해가 일어나서 *m/z* 145에서 가장 강도가 높은 피크를 만들었다. 반면에, GBPA의 음이온 스펙트럼은 *m/z* 312의 모분자 이온에서 CO_2와 NH=C=NH의 순차적인 중성 손실로 인하여 *m/z* 226의 가장 강도가 높은 피크가 특징적으로 생성되었다

Key words: camostat, 4-(4-guanidinobenzoyloxy)phenylacetic acid, serine protease inhibitor, ESI-MS/MS, CID

1. Introduction

Active synthetic serine protease inhibitors have been known to play important roles in many biological processes. *N*,*N*-dimethylcarbamoylmethyl 4-(4-guanidinobenzoyloxy)phenylacetate (camostat) (*Fig.* 1) is a synthetic proteolytic enzyme inhibitor for trypsin, plasmin, kallikrein, tissue kallikrein, and thrombin,[1] and has shown activity in the treatment of pancreatitis[2-6] and reflux esophagitis,[7, 8] establishing its safety for use in humans. Metabolic works have shown that camostat is rapidly hydrolyzed to 4-(4-guanidinobenzoyloxy)phenylacetic acid (GBPA) and 4-guanidinobenzoic acid (GBA) by esterases during intestinal absorption (*Fig.* 1).[13, 14] The protease inhibitory activity of GBPA is similar to that of camostat but GBA is inactive.[15]

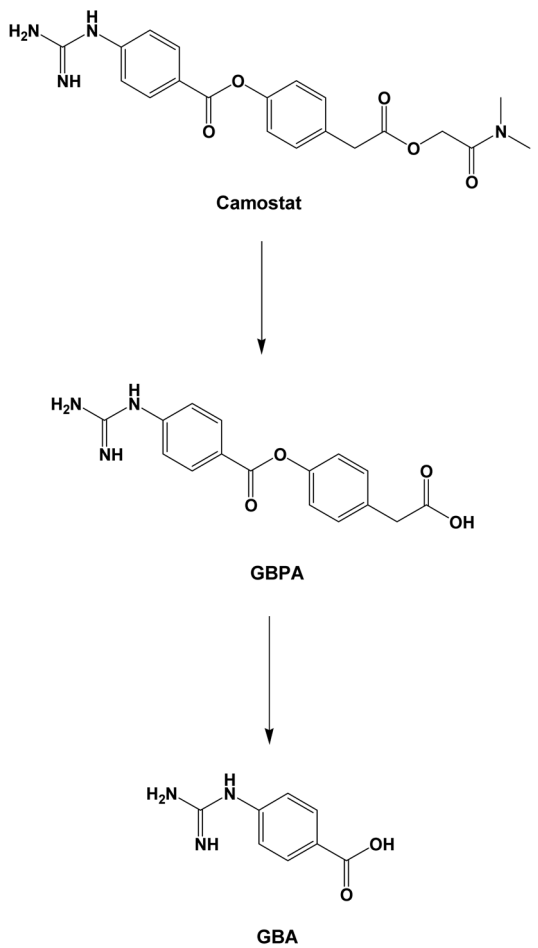

Fig. 1. Chemical structures of CM, GBPA, and GBA.

Electrospray ionization (ESI)-tandem mass spectrometry (MS/MS) has emerged as a primary analytical tool for the qualitative or the quantitative characterization of drug compounds.

ESI-MS/MS has widely been used to study fragmentation pathways of a variety of compounds with pharmaceutical activities.[16-22]

To date, studies of camostat and its degradation product, GBPA, have focused on their pharmacological effects.[9-12] A study on noncovalent interaction between camostat and cyclodextrin by ESI-MS has recently been reported.[23] However, no attempt has been made to investigate any of fragmentation patterns or pharmacokinetics of the two compounds by ESI-MS/MS. Therefore, establishment of fragmentation patterns of the two compounds will be needed to investigate pharmacokinetics or *in vitro* and *in vivo* metabolic screening of the compounds.

In the present work, we investigated the fragmentation behaviors of the protease inhibitor, camostat and its degradation product, GBPA by ESI-MS/MS in both positive and/or negative ion mode under low-energy CID.

2. Experimental Section

2.1. Materials

Camostat was from Ilsung Pharmaceuticals Co.,

Ltd. and GBPA was from Unites States Biological, Inc. Methanol of HPLC grade was used as a solvent.

2.2. Mass spectrometric measurements of camostat and GBPA

The samples were prepared by dissolving at 100 ng/mL in methanol. CID experiments were performed on an API 4000^{TM} triple quadrupole LC/MS/MS System (AB Sciex, Foster City, CA, USA) equipped with a turbo electrospray ion source. The sample solutions were directly infused into the ESI source with a flow rate of 10 mL/min. ESI mass spectra were measured at a scan range from *m/z* 50 to 500 with a spray voltage of 4500 V in the positive ion mode and from *m/z* 50 to 350 with a spray voltage of -4500 V in the negative ion mode. In the case of camostat, declustering voltage, entrance potential, collision energy and collision cell exit potential were 80 V, 10 V, 20 V and 12 V in the positive ion mode, respectively. In the case of GBPA, declustering voltage, entrance potential, collision energy and collision cell exit potential were 80 V or -80 V, 10 V or -10 V, 30 V or -20 V and 12 V or -12 V in the positive or negative ion mode, respectively. The pressures of N_2 as collision gas, curtain gas and ion source gas 1 were 6, 15 and 25 p.s.i., respectively. Selected ions for Q1 were *m/z* 399, which correspond to molecular masses $[M+H]^+$ of camostat, and *m/z* 314 and *m/z* 312, corresponding to $[M+H]^+$ and $[M-H]^-$ of GBPA, respectively.

3. Results and discussion

Abundant $[M+H]^+$ ions were produced when camostat was infused into the electrospray ion source and the ion current was stable during the infusion. Camostat was more amenable to MS/MS fragmentation in the positive ion mode than the negative. When subjected to CID in the positive ion mode, $[M+H]^+$ ion at *m/z* 399 yielded several fragment ions at *m/z* 382, 354, 296, 254, 162 and 104 as shown in *Fig.* 2a.

The relatively weak peaks at *m/z* 382 and 354 are resulted from the loss of NH_3 and $HN(CH_3)_2$ from

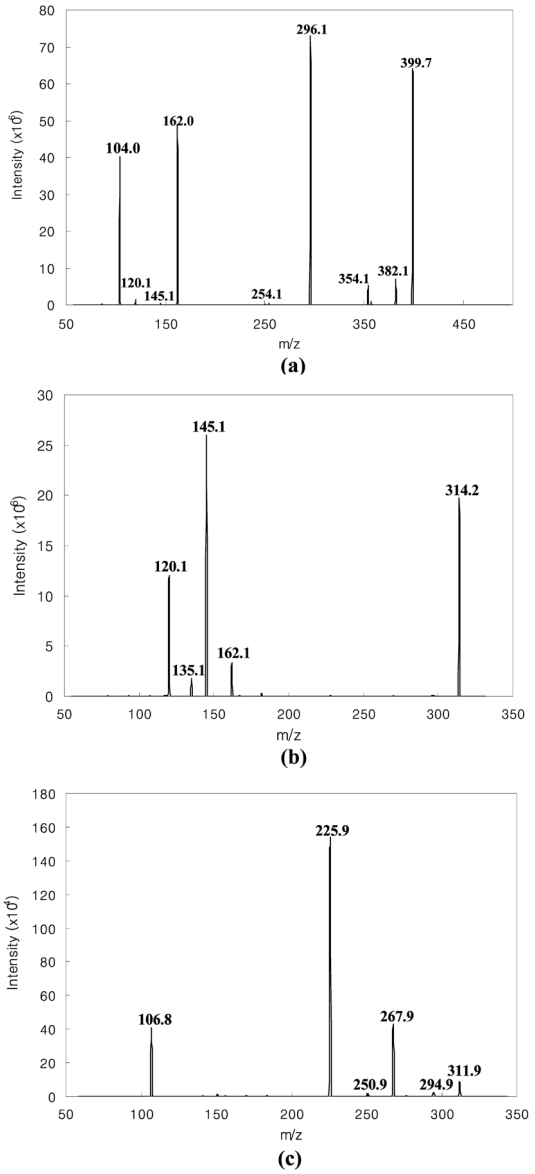

Fig. 2. ESI CID mass spectra of (a) camostat in the positive ion mode and of GBPA in the (b) positive and (c) negative ion mode.

$[M+H]^+$, respectively. Formation of the abundant base peak at *m/z* 296 is resulted from the loss of $OCH_2CON(CH_3)_2$ group from $[M+H]^+$ ion and the formation of the peak at *m/z* 162 is also formed by the C-O cleavage of the ester bond within guanidinobenzoyl group from $[M+H]^+$. The peak at *m/z* 162 was further fragmentized upon CID, giving rise

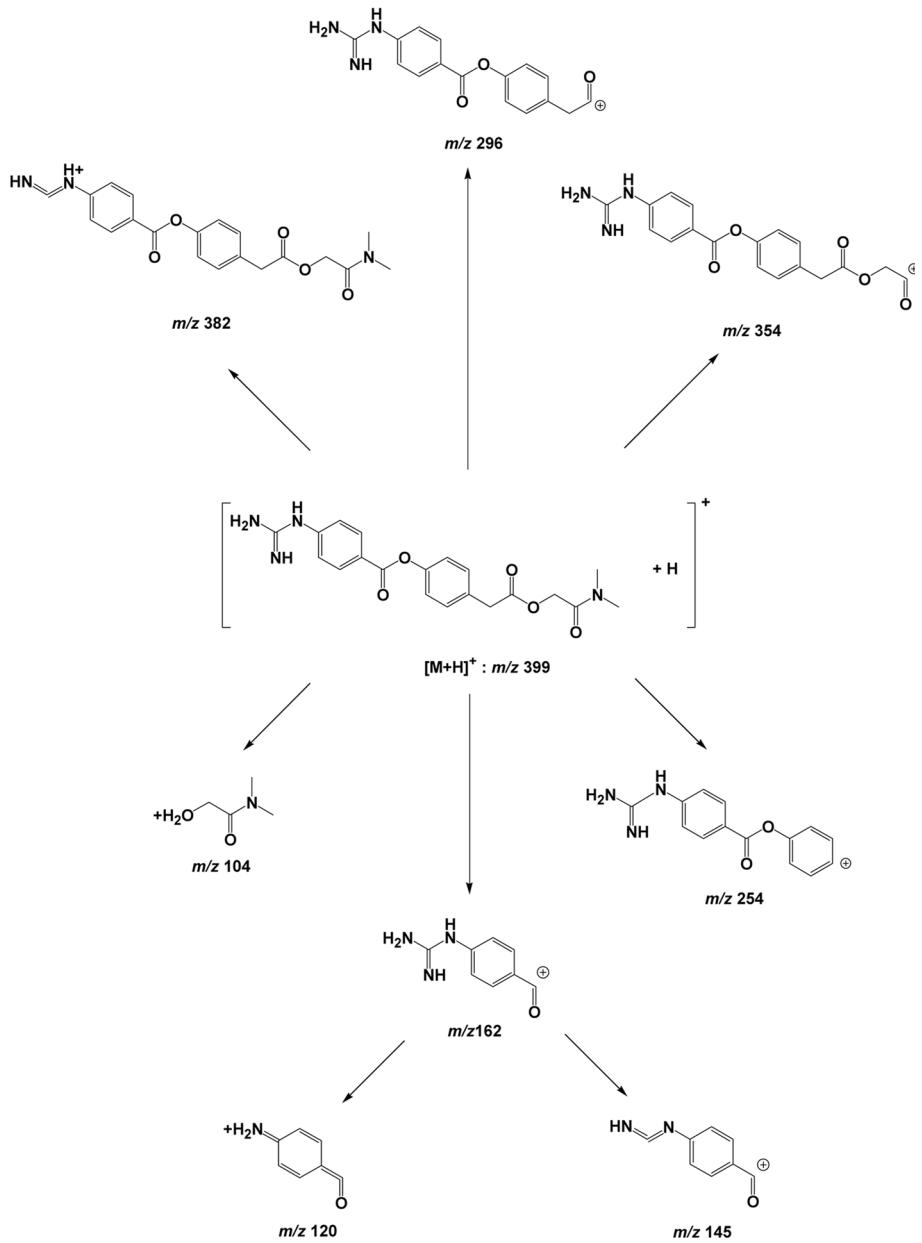

Fig. 3. Possible ESI CID mass fragmentation pattern of camostat in the positive ion mode.

to the two peaks at *m/z* 145 and 120 resulting from the loss of NH_3 and NH=C=NH from the guanidine group, respectively. The formation of the ion at *m/z* 104 from $[M+H]^+$ ion resulted from the C-O cleavage of the ester bond. The ion at *m/z* 104 indicated the presence of the protonated *N*,*N*-dimethylcarbamoylmethyloxy group (*Fig.* 3). The positive ion CID mass spectrum of camostat suggests that the loss of $OCH_2CON(CH_3)_2$ group resulting from the preferential C-O cleavage of the ester bonds was more susceptible than that of guanidine group, causing the formation of the intense peaks observed at *m/z* 296, 162 and 104. Interestingly, no any loss of guanidinium ions or of neutral guanidine was observed in positive ion

spectrum of camostat. The positive ion spectrum of camostat showed distinctly different fragmentation pattern with other general compounds containing guanidine group.[24, 25] Therefore, the CID spectrum shows that the C-O bond is the preferential cleavage site of camostat in the positive ion mode.

The CID fragmentation patterns of GBPA were less complex than those of camostat. When subjected to CID in the positive ion mode, GBPA was cleaved into just four fragmentation ions. The ions arising from the fragmentation of the parent ion at *m/z* 314 corresponding to $[M+H]^+$ is shown in *Fig.* 2b and *Fig.* 4.

The peak at *m/z* 135 with low intensity arised from the loss of guanidinobenzoyl group from the parent ion. Like camostat, the CID fragmentation spectrum of GBPA in positive ion mode was initiated by the cleavage of the C-O bond between the carbonyl group and the oxygen atom at guanidinobenzoyloxy moiety ($H_2NCNHNHC_6H_4COO$). The peak at *m/z* 162 arised from the cleavage of the ester bond linking the guanidinobenzoyl and the phenylacetate moiety and the ions yielded two intense ions at *m/z* 145 and 120. The most abundant peak at *m/z* 145 is resulted from the release of the NH_3 from guanidine group of the ion at *m/z* 162 and relatively intense ion at *m/z* 120 is arised from loss of HN=C=NH. No loss of the guanidine group was observed during low energy CID. These results indicate distinctly that the C-O bond at the ester group of GBPA is the primary cleavage site of the compound.

In negative ion mode, GBPA yielded parent ion $[M-H]^-$ at *m/z* 312 with weak intensity, one intense and base peak at *m/z* 226, two peaks with medium intensity at *m/z* 268 and 107, and the two peaks at *m/z* 295 and 251 with weak intensity when subjected to CID (*Fig.* 2c). The ions at *m/z* 268 and 295 are resulted from the losses of CO_2 and NH_3 from the parent ion $[M-H]^-$, respectively. The loss of CO_2 from the ion at *m/z* 295 led to the formation of the peak at *m/z* 251. Two peaks with weak intensity

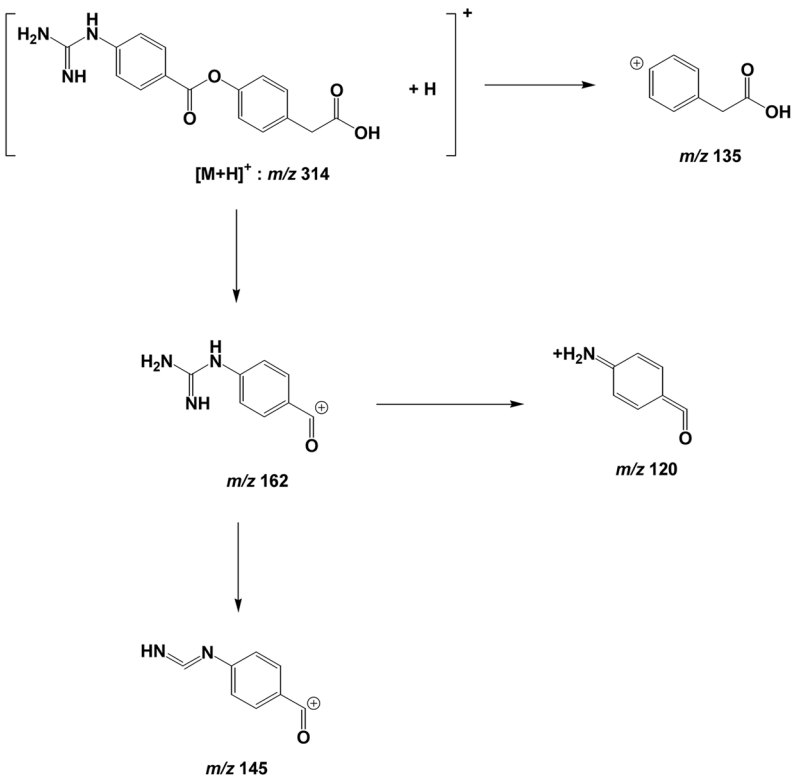

Fig. 4. Possible ESI CID mass fragmentation pattern of GBPA in the positive ion mode.

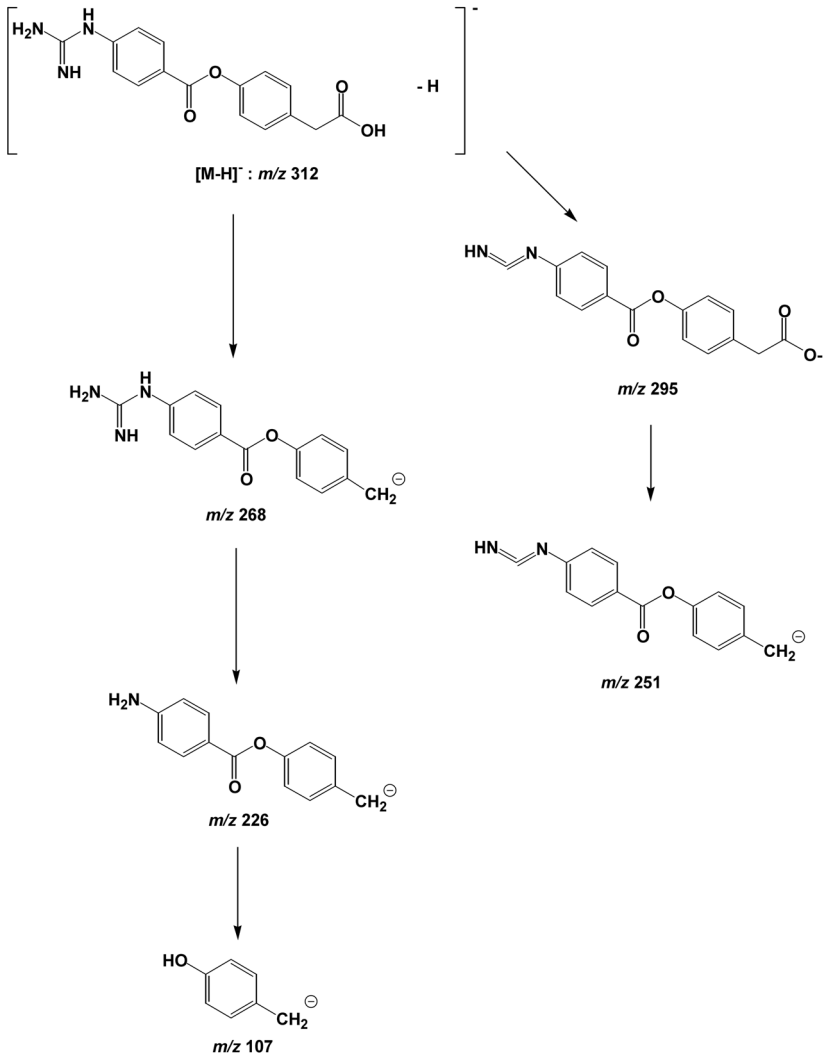

Fig. 5. Possible ESI CID mass fragmentation pattern of GBPA in the negative ion mode.

appeared at *m/z* 295 in which the ion is resulted from the loss of NH_3 from $[M-H]^-$ ion and at *m/z* 251 in which the ion is resulted from the loss of CO_2 from the one at *m/z* 295. The intense ion at *m/z* 226 is resulted from the losses of HN=C=NH and CO_2 from the ion at *m/z* 268. Finally, the peak with medium intensity at *m/z* 107 is resulted from the cleavage of the ester bond of the ion at *m/z* 226. The proposed fragmentation pattern of GBPA in negative ion mode is illustrated in *Fig.* 5. Thus, the negative CID spectrum of GBPA shows definitely that the fragmentation of the compound is preferentially initiated by the losses of CO_2 and NH_3 at both tips of the drug. Initial C-O bond cleavage at the ester bond of GBPA did not occur. This phenomenon was in contrast with the fragmentation patterns of camostat or GBPA in positive ion mode. These different CID mass spectrometric behaviors under low-energy CID probably can be attributed to the inherent structure of camostat or GBPA.

4. Conclusions

In positive and/or negative ion mode, low-energy

CID analysis by ESI-MS/MS was for the first time carried out to characterize the fragmentation patterns of camostat and its degradation product, GBPA. Camostat was more amenable to MS/MS fragmentation in the positive ion mode than the negative ion. The positive ion CID mass spectrum of camostat showed distinctively that the abundant ions at *m/z* 296, 162, and 104 are resulted from the C-O cleavage between carbonyl group and oxygen atom at the ester bonds. The molecular ion of GBPA was differently fragmented during the positive and negative CID. The positive ion spectrum of GBPA was also initiated by the cleavage of the C-O bond linking the carbonyl group and the oxygen atom at the ester bond of 4-guanidinobenzoyloxy moiety followed by the formation of four fragment ions. On the other hand, the fragmentation pattern of GBPA in the negative ion mode was characterized by the initial losses of NH_3 and CO_2 from the parent ion. In this study, the results will be helpful to further study pharmacokinetics of camostat or GBA and structural characterization of biologically active analogues similar to these compounds.

Acknowledgments

This work was supported by Seoul Medical Science Institute & Seoul Clinical Laboratories in 2010.

References

1. Y. Tamura, M. Hirado, K. Okamura, Y. Minato and S. Fujii, *Biochim. Biophys. Acta*, **484**(2), 417-422(1977).
2. N. Tanaka, R. Tsuchiya and K. Ishii, *Adv. Exp. Med. Biol.*, **120B**, 367-378(1979).
3. S. Takasugi, H. Yonezawa, N. Ikei and T. Kanno, *Digestion*, **24**(1), 36-41(1982).
4. M. Kanoh, H. Ibata, M. Miyagawa and Y. Matsuo, *Biomed. Res.,* **10**(suppl 1), 145-150(1989).
5. M. Kitagawa, S. Naruse, H. Ishiguro and T. Hayakawa, *Pancreas*, **16**(3), 427-431(1998).
6. M. Sugiyama, Y. Atomi, N. Wada, A. Kuroda and T. Muto, *J. Gastroenterol.*, **32**(3), 374-379(1997).
7. I. Sasaki, Y. Suzuki, H. Naito, Y. Funayama, Y. Kamiyama, M. Takahashi, T. Matsuo, K. Fukushima, S. Matsuno and T. Sato, *Biomed. Res.*, **10**(suppl 1), 167-173(1989).
8. I. Kobayashi, S. Ohwada, T. Ohya, T. Yokomori, H. Iesato and Y. Morishita, *Hepatogastroenterology*, **45**(20), 558-562(1998).
9. H. Sarles, *Scan. J. Gastroenterol.*, **6**(3), 193-198(1971).
10. H. Sarles, *Dig. Dis. Sci.*, **30**(6), 573-574(1985).
11. M. Okuno, K. Akita, H. Moriwaki, N. Kawada, K. Ikeda, K. Kaneda, Y. Suzuki and S. Kojima, *Gastroenterology*, **120**(7), 1784-1800(2001).
12. J. Gibo, T. Ito, K. Kawabe, T. Hisano, M. Inoue, N. Fujimori, T. Oono, Y. Arita and H. Nawata, *Lab. Invest.*, **85**(1), 75-89(2005).
13. K. Beckh, B. Goke, R. Muller and R. Arnold, *Res. Exp. Med. (Berlin),* **187**(6), 401-406(1987).
14. T. Nishihata, Y. Saitoh and K. Sakai, *Chem. Pharm. Bull. (Tokyo)*, **36**(7), 2544-2550(1988).
15. I. Midgley, A. J. Hood, P. Proctor, L. F. Chasseaud, S. R. Irons, K. N. Cheng, C. J. Brindley and R. Bonn, *Xenobiotica*, **24**(1), 79-92(1994).
16. X. Wang, Y. Sha, Z. Ge, W. Wang and R. Li. *Rapid Commun. Mass Spectrom.*, **25**, 349-354(2011).
17. M. Hubert-Roux, F. Bounoure, M. Skiba, P. Bozec, F. Churlaud and C. M. Lange. *J. Mass Spectrom.*, **45**, 1121-1129(2010).
18. M. Marull and B. Rochat. *J. Mass Spectrom.*, **41**, 390-404(2006).
19. M.-Y. Zhang, N. Pace, E. H. Kerns, T. Kleintop, N. Kagan and T. Sakuma. *J. Mass Spectrom.*, **40**, 1017-1029(2005).
20. X. Wang, Y. Sha and R. Li. *Int. J. Mass Spectrom.*, **235**, 111-115(2004).
21. Z. Tozuka, H. Kaneko, T. Shiraga, Y. Mitani, M. Beppu, S. Terashita, A. Kawamura and A. Kagayama. *J. Mass Spectrom.*, **38**, 793-808(2003).
22. H. Wang, Y. Wu and Z. Zhao. *J. Mass Spectrom.*, **36**, 58-70(2001).
23. S. Kwon, W. Lee, H. Shin, S. Yoon, Y. Kim, Y. Kim, K. Lee and S. Lee. *J. Mol. Struct.,* **938**, 192-197(2009).
24. M. W. Forbes, R. A. Jockusch, A. B. Young and A. G. Harrison. *J. Am. Soc. Mass Spectrom.,* **18**, 1959-1966 (2007).
25. P. M. Gehrig, P. E. Hunziker, S. Zahariev and S. pongor. *J. Am. Soc. Mass Spectrom.,* **15**, 142-149(2004).